P-wave anisotropy in shales from crosswell data

Jerry M. Harris*, *Stanford University;* Leon Dahlhaus, *University of Utrecht;* and Reinaldo Michelena, *Stanford University*

SL3.3

SUMMARY

A crosswell dataset, collected at Conoco' s Borehole Test Facility in Oklahoma, was first processed using a tomography algorithm based on ***an isotropic*** velocity model. The resulting 2-D velocity tomogram was found to have huge artifacts believed to be caused by nonuniform ray coverage and possibly anisotropy. A comparison of the zero offset crosswell velocities (Horizontal Path Log) with the log-derived sonic velocities (Vertical Path Log) indicated nearly 25% P-wave anisotropy in some formations. Despite the artifacts, a good interpretation of the 2-D isotropic tomogram was made with the help of synthetic data. The data were then inverted using an algorithm that incorporates a model of elliptical transverse isotropy. This *anisotropy* model produced an unambiguous image for two components of velocity that simultaneously match the sonic log and the crosswell data. Both inversions support a final interpretation of 1-D vertical stratification of layers, some of which exhibit significant P-wave anisotropy. This interpretation is consistent with the sonic logs, crosswell data, and available geological information.

INTRODUCTION

Crosswell seismic tomography has been successfully used for reservoir delineation in carbonate reservoirs (Harris et al, 1992; Lines et al, 1993). In these cases, few problems were caused by velocity anisotropy and the tie between the tomogram and the well logs was reasonably good. This does not hold true for shales and clastic reservoirs (Harris et al, 1990) or for the Newkirk site described in this paper. A few recent reports have discussed observations of anisotropy in crosswell field data (Miller, 1992; Onishi and Harris, 1991).

The data described here were recorded in September 1991 between two wells at Conoco' s Borehole Test Facility (CBTF) near Newkirk in Kay County, Oklahoma. The objective of the study was to apply traveltime tomography to image vertical stratification and possibly identify zones of natural fracturing with shear waves if present. An unanticipated result was the large degree of P-wave anisotropy found in some layers. This P-wave anisotropy was first suspected from artifacts introduced by an inversion algorithm based on isotropic media. The effect of anisotropy was verified by processing a synthetic dataset generated for a transversely isotropic model. The field data were then reprocessed using an inversion model with transverse isotropy (Michelena et al, 1993). This paper describes the geological setting, data processing and the interpretation of the tomograms.

SITE DESCRIPTION

The Conoco Borehole Test Facility is located in the north central part of Oklahoma. There are several boreholes at the site and for this survey the Conoco 33-5 and Conoco 33-6 were used. A complete suite of wireline logs indicate that the layers in the CBTF area are flat-lying. The geologic setting is sedimentary with mostly horizontally layered sandstones, shales and some limestones. There are no structurally complex features with the possible exception for three sets of subsurface vertical fractures (Queen and Rizer, 1990): a NE striking set, a ENE striking set and a ESE striking set. The fracturing has no apparent correlation with depth or stratigraphy, but has been shown to cause subtle shear wave anisotropy in VSP data.

The well heads of Conoco 33-5 and Conoco 33-6 are 400.5 ft apart (FIG. 1) with an azimuth bearing generally ESE. The total deviation with depth of the Conoco 33-5 never exceeds one foot whereas the Conoco 33-6 well is slightly deviated. The primary target zone of the tomography survey lies between depths of 1900 ft and 2760 ft. The nominal separation of the two boreholes at the target depth is about 404 ft where the well starts deviating in a WNW direction at a depth of 2560 ft. At 2760 ft the well spacing is approximately 3 84 ft. Nominal borehole diameter is 8.5 inches. There is no casing.

DATA ACQUISITION

The Conoco 33-5 was used for the source and Conoco 33-6 for the receivers. Stanford's piezoelectric bender was used as the downhole source. A sweep signal with a length of 250.0 ms and start-stop frequencies of 300 Hz and 2400 Hz, respectively, was chosen. Thirty-two sweeps were stacked to form the recorded seismic trace. A 6-element hydrophone array was used as receivers. The individual hydrophones were spaced 10 ft apart. The data were sampled at 100 microsecond with 4096 samples per trace. A total of 10 common receiver fans were recorded. Receiver points covered a depth range from 2760 ft to 2230 ft also at lo-ft intervals. The typical shooting pattern fixed the receiver array and scanned the source upwards from 2750 ft to 1900 ft at ten-foot intervals (FIG. 1). Fan 8 (receiver depths 2230 ft to 2280 ft) was shot at a five-foot source interval by interleaving lo-ft scans. In general, the recording aperture ranged from approximately +65/+10 degrees for the deepest receivers to +40/-50 degrees for the shallowest. Fans 9 and 10 (receiver depths 2475 ft to 2625 ft) could not be used because of errors in their depth position, probably as a result of mud in the borehole making it difficult to

interleave the receiver array between previously recorded depths. The remaining eight fans together provided about 5 150 traces of which 4969 were used for tomography and analysis. A typical common-source gather is shown in FIG. **2.**

HORIZONTAL PATH VS. VERTICAL PATH LOGS

It is known that *P-wave* anisotropy can occur in laminated shales. The sonic logs give a good indication of velocity along vertical paths (Vertical Path Log). In a thick and laterally homogeneous layer, the zero vertical offset crosswell traces (source and receiver at the same depth) provide an estimate for the velocities between the two wells along horizontal paths (Horizontal Path Log). The latter is made using the first arrival times and the correct values for the separation of the boreholes. The median filtered sonic velocities at the two wells are compared with the zero offset crosswell velocities in FIG. 3. The most striking difference in this comparison can be seen at depths between 2500 and 2700 ft. In this interval, the average horizontal velocity from the crosswell log is approximately 15000 ft/s and the vertical velocity from the sonic log is about 11500 ft/s. The crosswell estimate is approximately 30% faster than the log estimate. The high values in the SP, gamma ray and calculated porosity logs as well as the mud reports for this interval indicate a thick shale formation.

ISOTROPIC TRAVELTIME TOMOGRAPHY

Picking was done on both common shot gathers (CSGs) and common receiver gathers (CRGs) as well as on common (vertical) offset gathers (COGS). The final result was a set of 4969 gather-consistent arrival times. The picked traveltimes were then inverted to solve for the interwell velocity. The string inversion algorithm was used with a constant starting velocity (Harris, 1991). This algorithm produces a model of 1-D or 2-D isotropic velocity. FIG. 4a shows the 2-D tomogram of compressional wave velocities after 10 iterations with a constant velocity (14200 ft/s) starting model. The mean absolute residual traveltime error is less than 1 millisecond. Examination of this 2-D *isotropic* tomogram clearly shows poorly imaged areas: the triangular shaped region in the upper part of the image and the arc-like feature at the bottom. These are due to the asymmetrical ray coverage and missing data. As a result, only the middle part of the tomogram (2200-2700 ft) can be reliably used for visual interpretation, even though this section has large artifacts too. Furthermore, comparison of the isotropic tomogram and the sonic logs shows poor correlation. Only the low velocity sandstone zone at a depth of approximately 2400 ft appears to match.

To test the hypothesis that anisotropy and ray coverage were reponsible for the poor tomogram obtained from the field data, we created two synthetic traveltime datasets for inversion, one isotropic, the other anisotropic. The isotropic synthetic model was derived from the zero vertical offset crosswell velocities. A 1D raytracer was used to create the synthetic traveltimes. The same inversion procedure used on the field data was applied to this isotropic model dataset. The velocities were reconstructed very well and only the geometry and coverage problems near the edges were found to cause artifacts.

We then created a synthetic dataset using a model with 1-D transverse isotropy and performed the isotropic inversion again. The model assumed elliptical anisotropy with the two velocity components taken from FIG. 4. In order to identify the artifacts related to missing data and asymmetrical coverage, we created subsets of the synthetic data to exactly match the field survey. The resulting synthetic tomogram is shown in FIG. 4b. Comparing the tomogram made with the anisotropic synthetic with the tomogram made from the field data, one sees remarkable similarities, especially in the lower shale section below 2500 ft. Such similarities were not present in the isotropic synthetic (not shown), thus providing strong evidence of anisotropy in the thick lower shale. The use of the synthetic is an excellent way of obtaning an interpretation of the field data tomograms, even when anisotropic inversion tools are not avalible. We conclude that anisotropy and non-uniform ray coverage contribute the huge artifacts to the field data tomogram created with the isotropic algorithm (FIG. 4a).

ANISOTROPIC TRAVELTIME TOMOGRAPHY

A better method of estimating the magnitude of the anisotropy is to use an inverse model that includes anisotropy. We chose an elliptical model with variable axis of symmetry to describe the variations of velocity with direction and a layered structure (with dipping straight interfaces) to describe the heterogeneities (Michelena, et al, 1993). The data were inverted iteratively starting from a homogeneous isotropic model with 130 horizontal layers and a vertical axes of symmetry. Ray bending at the interfaces was properly considered by tracing rays in the TI model. The starting values of slopes of the boundaries and axes of symmetry of the different layers didn't change significantly through the iterations and therefore, the final model also has horizontal layers with vertical axes of symrnetry.

FIG. 5 shows the estimated horizontal and vertical components of velocity estimated for the TI model. Because the velocity model is assumed to be elliptical, the estimated vertical component corresponds to the value of a best fitting ellipse, i.e., $V_{z\text{-}nmo}$, whereas the horizontal component is a true velocity. The sonic log velocity, blocked to 7 ft, is displayed with the tomogram velocities. The large anisotropy (-25%) of the interval between 2500 ft and 2700 ft is consistent with the values estimated from the Horizontal Path log.

More importantly, the vertical component of the TI velocity model is closer to the sonic log than the horizontal component. Therefore, using an elliptical model for the velocities appears appropriate. Note, however, that the estimated vertical component is

consistently less than or equal to to the log value, which means that the true anisotropy may not be elliptical. In the interval between 2500 and 2700 ft, $V_{z\text{-}nmo}$ alternates between being equal and lower than the log velocity, another feature which suggests that this interval may be a combination of different layers with varying degree of non-elliptical anisotropy.

CONCLUSIONS

This study shows that significant P-wave anisotropy can be present in sedimentary shales. This type of anisotropy is likely due to thin bed laminations, through which horizontally propagating waves travel faster than vertically propagating waves. The anisotropy, in this case greater than 25%, gives rise to hugh artifacts in tomograms generated by isotropic allgorithms. Nevertheless, we have shown that in this simple sedimentary environment a good model of the stratified heterogeneity could be found with the use of the sonic logs and zero vertical offset velocities. Because the isotropic inversion method is not suitable for imaging anisotropic media, the use of well logs, geological information, and synthetic traveltime models is necessary to be able to interpret the inversion results. The remarkably good comparison between the field data tomogram and the synthetic data tomogram may be called an interpretative isotropic inversion.

The data were inverted for a model of elliptical anisotropy. This transversely isotropic model leads to a consistent interpretation of the crosswell and the log data, further supporting a model of strong P-wave anisotropy at the Newkirk site. This inversion gave a much better match to the logs and a model fully consistent with the interpretative isotropic model discussed above.

ACKNOWLEDGMENTS

The authors thank Conoco, Inc. for their sponsorship of this study and for granting permission to publish this paper. Special thanks to John Queen, John Sinton, Bill Rizer, Dale Cox and others of the crosswell team for their cooperative support of the project.

REFERENCES

Harris, J. M., 1990. Tomographic string inversion, Expanded Abstracts of the SEG Annual Meeting, pp. 84-88.

Harris, J. M., L. Lines, H. Tan, G. Mavko, D. Moos, C. Pearson, R. Nolen-Hoeksema, and S. Treitel, 1990. Crosswell tomographic imaging of geological structures in gulf coast sediments, Expanded Abstracts of the SEG Annual Meeting, p. 37.

Lines, Lawrence, et. al, 1993. Integrated Reservoir Characterization: Beyond tomography, Expanded Abstracts of the SEG Meeting, p. 298.

Michelena, R. J., F. Muir, and J. M. Harris, 1993. Anisotropic traveltime tomography, Geophysical Prospecting 41, 1993, p. 381-412.

Miller, D. E. and C. H. Chapman, 199 1. Incontrovertible evidence of anisotropy in crosswell data, Expanded Abstracts of the SEG Annual Meeting, p. 825.

Onishi, M. and J. M. Harris, 1991. Anisotropy from head waves, Expanded Abstracts of the SEG Annual Meeting, p. 115.

Queen, J.H. and W. D. Rizer, 1990, Seismic Anisotropy and Natural Fractures, Journal of Geophysical Research, 95-97, 11.255-11.273

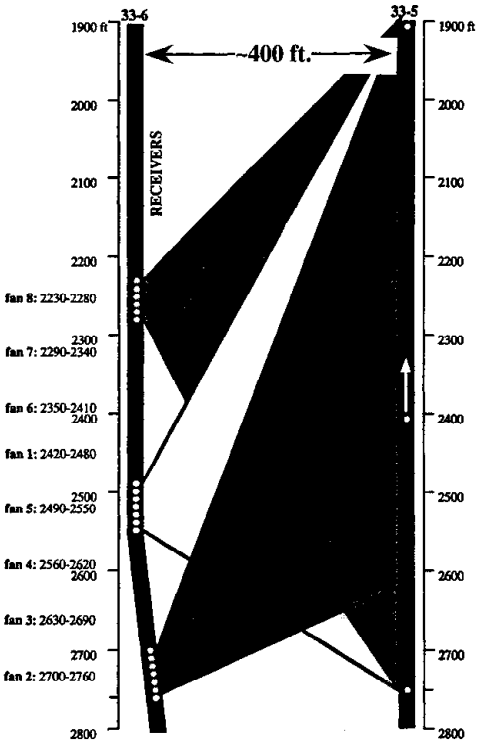

FIG. 1. Shooting patterns; receiver spacing 10 ft, shot interval 10 ft (fan l-7) or 5 ft (fan 8).

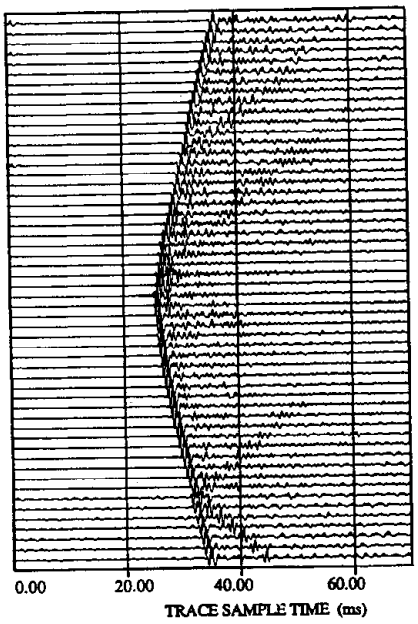

FIG. 2. Common shot gather at shot depth 2500 ft.

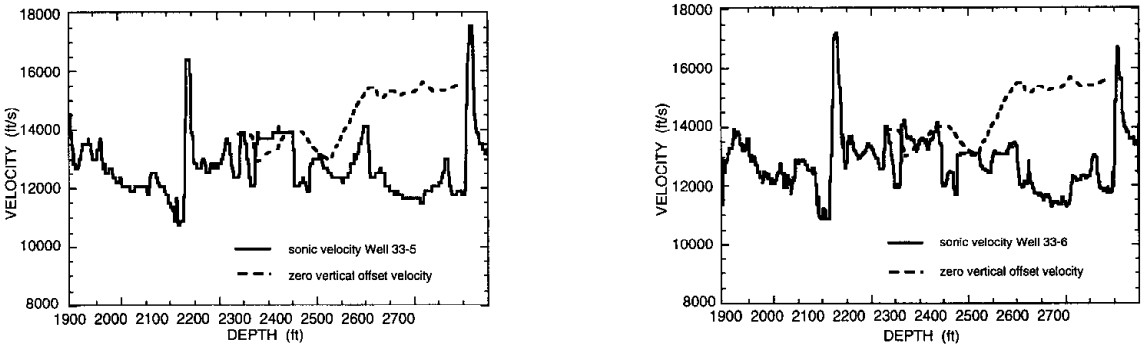

Fig. 3. Comparison of sonic log velocity (Vertical Path Log) and zero vertical offset crosswell velocity (Horizontal Path Log).

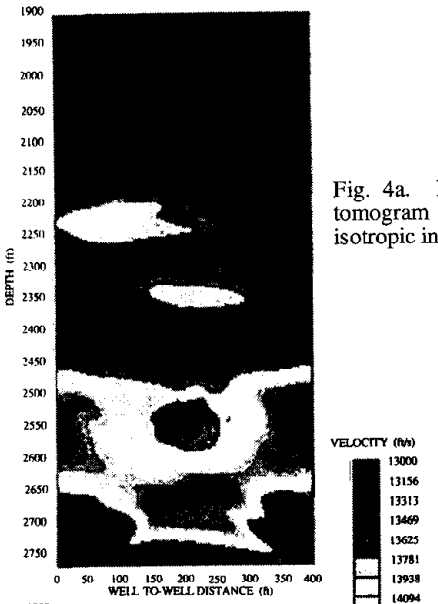

Fig. 4a. Field data *P*-wave tomogram created with an isotropic inversion model.

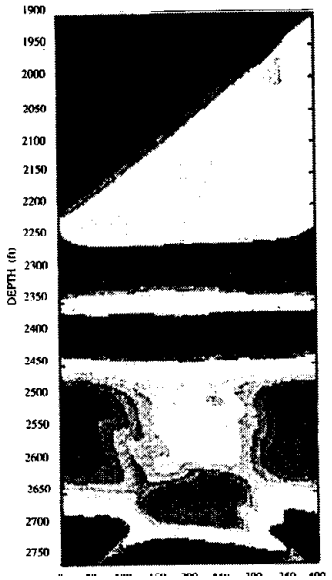

Fig. 4b. Synthetic data *P*-wave tomogram created with an isotropic inversion model.

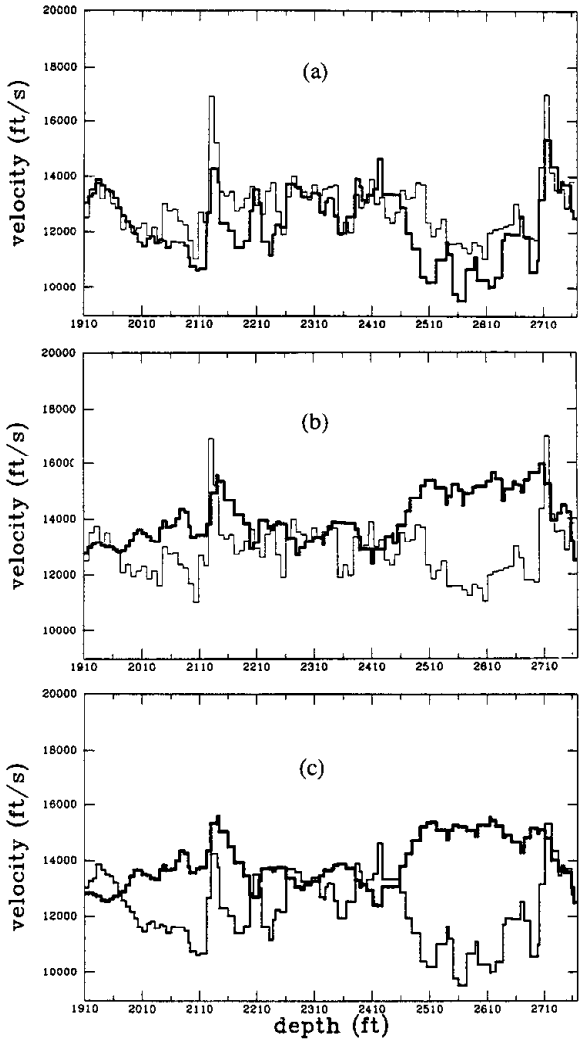

Fig. 5. Result of 1-D transverse isotropy inversion. (a) horizontal component (V_x, thick line); vertical component ($V_{z\text{-nmo}}$, thin line). Comparison between estimated horizontal component of velocity (thick line) and the sonic log (thin line). (c) Comparison between the estimated vertical velocity (thick line) and the sonic log velocity (thin line).